

Laboratory
of
ELECTROMAGNETIC THEORY

AD 647 695

Square Van Atta reflector with or
without a conducting plate.

Tove Larsen and Erik Dragø Nielsen

Scientific Report No.5
Contract AF61(052)-794

S127 R53
August 1966

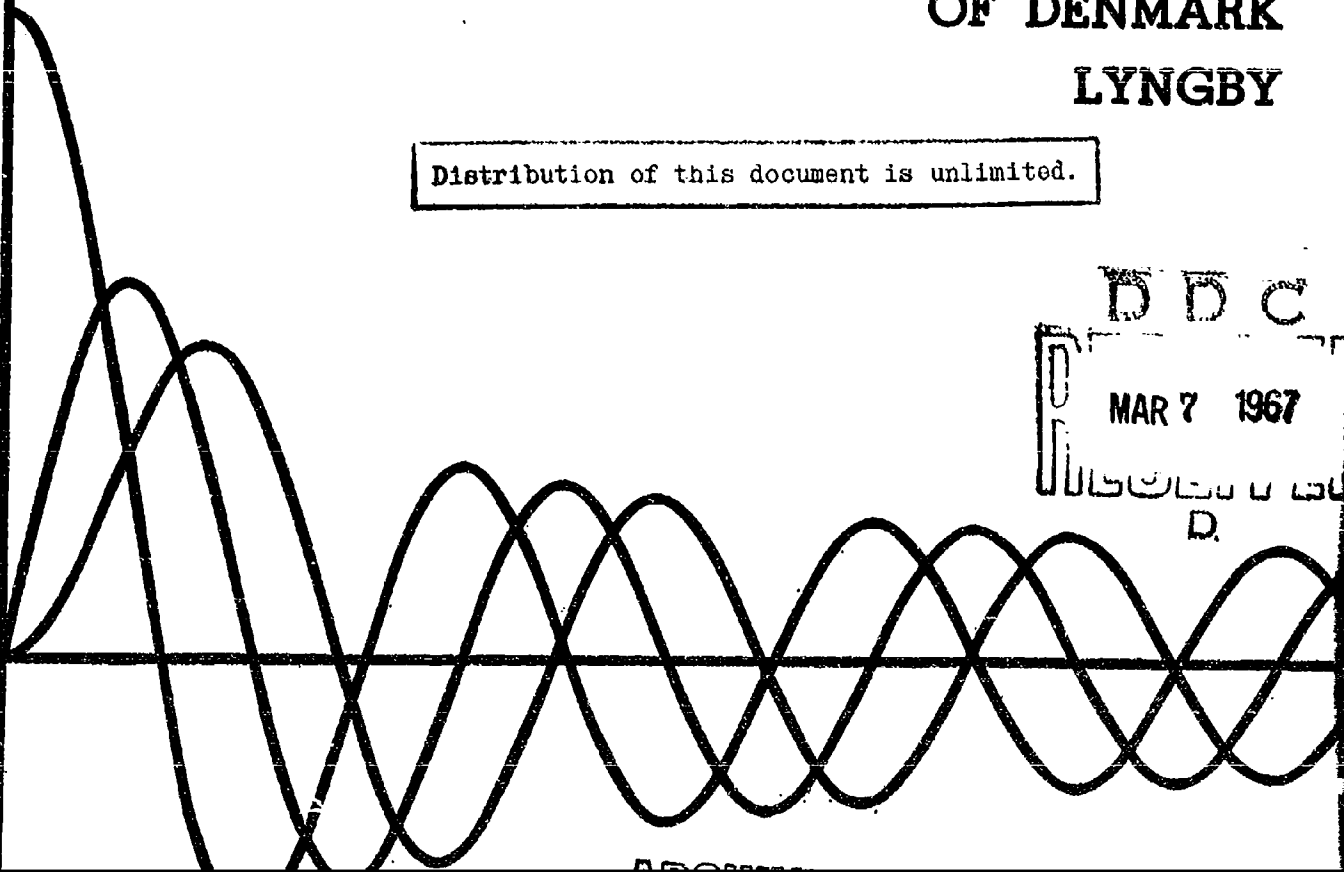
THE TECHNICAL UNIVERSITY
OF DENMARK
LYNGBY

Distribution of this document is unlimited.

DDC

MAR 7 1967

RESERVED
D.



Square Van Atta reflector with or
without a conducting plate.

Tove Larsen and Erik Dragø Nielsen

Scientific Report No.5
Contract AF61(052)-794

S127 R53
August 1966

Distribution of this document is unlimited.

The research reported in this document has been sponsored
by the AIR FORCE CAMBRIDGE RESEARCH LABORATORIES, OAR under Contract
AF 61(052)-794 through the European Office of Aerospace Research, (OAR),
United States Air Force.

ABSTRACT

A theoretical investigation of a square Van Atta reflector consisting of half wave dipoles mounted above and parallel to a conducting plate has been carried out. Each pair of antenna elements is represented by an equivalent circuit, using π -circuits for the transmissionlines. The mutual impedance between the antenna elements and the reradiation both from the elements and from the plate is taken into account. The influence of the conducting plate is treated by using the theory of images. The scattering cross section of the reflector has been examined analytically and numerically. The numerical results are compared with experimental results obtained by others.

TABLE OF CONTENTS

Abstract	
1. Introduction	3
2. Theoretical investigation	4
2.1 Way of approach	4
2.2 Induced voltage	5
2.3 Self- and mutual impedances	6
2.4 Field reflected from the conducting plate	7
2.5 Field reradiated from the Van Atta reflector and its image	9
2.6 Total reradiated field	10
3. Numerical results	12
3.1 Description of the properties of the reflector system	12
3.2 Comparison with results obtained by Sharp	13
3.3 Effect of changing the parameter values	14
3.4 Effect of turning the plane of incidence	16
4. Conclusion	17
5. References	18

Figures

1. INTRODUCTION

In the previous scientific reports 1,2,3,4)* under this contract, investigations have only dealt with simple linear or square reflectors. Thus the effect of mounting the dipoles above and parallel to a conducting plate has not been taken into account. The method of investigating a two-dimensional Van Atta reflector with a conducting plate is briefly described in section 6 of the Annual Summary Report 5).

It is the purpose of this report to describe an analytical and numerical treatment of square Van Atta reflectors with a conducting plate. The scattering cross section of such reflectors will be calculated and the influence of the distance between adjacent elements, the distance between the elements and the plate, the length and the characteristic impedance of the transmission-lines, and the number of elements will be discussed.

Furthermore a comparison will be made between the numerical results of this investigation and the experimental results obtained by Sharp 6) for a square Van Atta reflector consisting of 16 dipole elements mounted parallel to and a quarter of a wavelength above a conducting plate.

* In the following referred to as SR1, SR2, SR3, and SR4, respectively.

2. THEORETICAL INVESTIGATION

2.1 Way of approach.

The system investigated is shown in fig. 1. The antenna elements are half-wave dipoles placed in the xy -plane and parallel to the y -axis in a square configuration. A square perfectly conducting plate is placed parallel to and at a distance h below the xy -plane (the plane of dipoles).

A problem involving a conducting plate suggests itself to be treated by the theory of images. However this theory requires a conducting plate of infinite extent, which is not present in the actual problem. Furthermore it is wanted to use the same procedure and the same computer program for the reflector with a plate as for the reflector without a plate. This leads to a way of approach, which is similar to the use of the theory of images, but the course of the computations is chosen such that they follow the method of investigation used in SR1.

A sketch of the reflector is shown in fig. 2a. Using the theory of images the configuration shown in fig. 2b is obtained. The total voltages induced in corresponding elements of the two simple reflectors from the two primary plane waves are equal but of opposite sign. This means that also the currents in corresponding elements will be equal but of opposite sign.

The equations (17) and (18) of SR1 will on the right hand side be supplemented with the sums

$$- \sum_{\substack{n=1 \\ n \neq m, k}}^N i_n (z'_{nm} - z'_{nk}) \cos \frac{ka}{2} \quad (1)$$

and

$$- \sum_{\substack{n=1 \\ n \neq m, k}}^N i_n (z'_{nm} + z'_{nk}) \sin \frac{ka}{2} \quad (2)$$

respectively, where z'_{nm} is the normalized mutual impedance between element number n of the array and element number m of the image array.

The new sums (1) and (2) may be incorporated in the formerly used equations (17) and (18) of SRL so that these are unchanged, except that the self- and mutual impedance take the new values:

$$Z_{A,plate} = Z_A - Z'_{nn} \quad (3)$$

$$Z_{mk,plate} = Z_{mk} - Z'_{mk} \quad (4)$$

These are the impedance values of antennas over a conducting plate as shown in section 2.3.

The total reradiated field will be found as the sum of the fields reradiated from the simple dipole reflector itself, the image dipole reflector, and the conducting plate.

2.2 Induced voltage.

The open-circuit voltage induced in the dipoles will be given by

$$V = \vec{E} \cdot \vec{L}_{eff} \quad (5)$$

where \vec{E} is the electric field strength at the position of the element and \vec{L}_{eff} is the effective length of the antenna element as given in formula (4) in SRL.

For a half-wave dipole parallel to the y-axis we have

$$\vec{L}_{eff} = \frac{\lambda}{4\pi} \frac{\cos(\frac{\pi}{2} \cos u)}{\sin u} \hat{y} \quad (6)$$

where u is the angle between the direction of the dipole and the direction of propagation of the primary plane wave. With our notation (see fig. 1) we have that u is given by

$$\cos u = \sin\theta_1 \sin\phi_1. \quad (7)$$

The electric field strength is found from ordinary reflection theory. The primary plane wave is decomposed into two plane waves, one polarized in the plane of incidence and the other perpendicular to the plane of incidence. Each of these give rise to two components of field strength in the plane of dipoles, one from the primary wave and one from the reflected wave. We thus obtain

$$\begin{aligned}
\bar{E}(x,y,0) = & E_0 \cos v \left[(-\cos\theta_1 \cos\phi_1 \hat{x} - \cos\theta_1 \sin\phi_1 \hat{y} + \sin\theta_1 \hat{z}) e^{-ik\sin\theta_1(x\cos\phi_1 + y\sin\phi_1)} \right. \\
& + (\cos\theta_1 \cos\phi_1 \hat{x} + \cos\theta_1 \sin\phi_1 \hat{y} + \sin\theta_1 \hat{z}) e^{-ik(\sin\theta_1(x\cos\phi_1 + y\sin\phi_1) - 2h\cos\theta_1)} \left. \right] \\
& + E_0 \sin v \left[(-\sin\phi_1 \hat{x} + \cos\phi_1 \hat{y}) e^{-ik\sin\theta_1(x\cos\phi_1 + y\sin\phi_1)} \right. \\
& + (\sin\phi_1 \hat{x} - \cos\phi_1 \hat{y}) e^{-ik(\sin\theta_1(x\cos\phi_1 + y\sin\phi_1) - 2h\cos\theta_1)} \left. \right]. \quad (8)
\end{aligned}$$

By substituting equations (6) and (8) in equation (5) we obtain the following expression for the open-circuit voltage in the dipoles

$$\begin{aligned}
V = & E_0 \frac{2\lambda}{\pi} \frac{\cos(\frac{\pi}{2} \cos u)}{\sin u} (\cos v \cos\theta_1 \sin\phi_1 - \sin v \cos\phi_1) \\
& \sin(kh \cos\theta_1) e^{i(\frac{\pi}{2} + kh \cos\theta_1)} e^{-ik\sin\theta_1(x\cos\phi_1 + y\sin\phi_1)}.
\end{aligned}$$

2.3 Self- and mutual impedances.

In SRL the following expressions for the self-impedance Z_A of a dipole antenna and the mutual impedance Z_{12} between two dipole antennas were given

$$Z_A = - \int_0^L \frac{I_1(z) E_z(z)}{I_1^2} dz \quad (9)$$

$$Z_{12} = - \int_0^{L_2} \frac{I_2(z) E_{z21}(z)}{I_1 I_2} dz. \quad (10)$$

A figure and an explanation of the notation may be found in SRL p 8-9.

These formulas are still valid when the conducting plate is present, but the values of the electric field strengths E_z and E_{z21} have to be changed due to the presence of the plate, see figs. 2a and 2b.

Using the theory of images we see that the electric field strength E_{z1} at the position of antenna 1 due to its own current I_1 has to be supplemented by the electric field strength E_z image radiated by its image antenna to obtain the self impedance of the dipole antenna:

$$\begin{aligned}
Z_{A,plate} &= - \int_0^L \frac{I(z) [E_{z1}(z) + E_{z \text{ image}}(z)]}{I_1^2} dz \\
&= - \int_0^L \frac{I(z) E_{z1}(z)}{I_1^2} dz + \int_0^L \frac{I(z) E_{z \text{ image}}(z)}{I_1 I_1 \text{ image}} dz \\
&= Z_A - Z'_{11} \tag{11}
\end{aligned}$$

where Z'_{11} is the mutual impedance between the antenna and its image antenna, and $I_1 \text{ image} = -I_1$.

Correspondingly we obtain for the mutual impedance between two dipole antennas when the conducting plate is present:

$$\begin{aligned}
Z_{12,plate} &= - \int_0^{L_2} \frac{I_2(z) [E_{z21}(z) + E_{z2(\text{image of 1})}(z)]}{I_1 I_2} dz \\
&= - \int_0^{L_2} \frac{I_2(z) E_{z21}(z)}{I_1 I_2} dz + \int_0^{L_2} \frac{I_2(z) E_{z2(\text{image of 1})}(z)}{I_1 I_2 \text{ image}} dz \\
&= Z_{12} - Z'_{12} \tag{12}
\end{aligned}$$

where Z'_{12} is the mutual impedance between the image of antenna 1 and antenna 2, and $I_2 \text{ image} = -I_2$.

2.4 Field reflected from the conducting plate.

In order to find the field reflected from the plate itself we will use the method of physical optics given f.ex. in Kerr's book ⁹⁾ where the back-scattering cross section of a rectangular plate is given for a plate the dimensions of which are not small compared to the wavelength. The reflecting properties of the plate are supposed not to be influenced by the presence of the dipoles.

The reradiated field is found from the surface current distribution \vec{K} on the plate. This current is assumed to be the same as if the plate was infinite in extent.

Under this assumption the total tangential magnetic field is

$$\begin{aligned} \vec{H}_{\text{tot}}^t = \frac{2E_0}{\zeta_0} e^{ikx \cos \theta_i} \cdot e^{-ik \sin \theta_i (x_p \cos \phi_i + y_p \sin \phi_i)} \\ [x(-\cos v \sin \phi_i + \sin v \cos \theta_i \cos \phi_i) \\ + y(\cos v \cdot \cos \phi_i + \sin v \cdot \cos \theta_i \sin \phi_i)] \end{aligned} \quad (13)$$

and the surface current is

$$\vec{K} = \hat{z} \times \vec{H}_{\text{tot}}^t \quad (14)$$

(An explanation of the notation may be found in figs. 1 and 3).

The vector potential of the surface current is

$$\vec{A} = \frac{\mu}{4\pi} \int_{\text{plate}} \vec{K} \frac{e^{ikR_p}}{R_p} d\alpha \quad (15)$$

where R_p is the distance from the plate to the field point as shown in fig. 3. The electric field reflected from the plate may now be expressed as

$$\vec{E}_{\text{plate}} = i\omega \vec{A} \quad (16)$$

By using the far field approximations for R_p in equation (15), which according to fig. 3 means:

$$\begin{aligned} R_p &\approx R - \vec{r}_p \cdot \hat{p} + h \cos \theta && \text{in the numerator and} \\ R_p &\approx R && \text{in the denominator,} \end{aligned}$$

we obtain the following expression for the field reradiated from the plate:

$$\begin{aligned} \bar{E}_{\text{plate}}(R, \theta, \phi) &= \frac{i\omega\mu E_0}{2\pi \zeta_0} \cdot \frac{e^{ikR}}{R} \cdot e^{ikh(\cos\theta_i + \cos\theta)} \cdot b \cdot c \\ &\cdot \frac{\sin\alpha}{\alpha} \cdot \frac{\sin\beta}{\beta} \{ \hat{\theta} [-(\cos v \cdot \cos\phi_i + \sin v \cdot \cos\theta_i \cdot \sin\phi_i) \\ &\cdot \cos\phi \cos\theta + (-\cos v \cdot \sin\phi_i + \sin v \cdot \cos\theta_i \cdot \sin\phi_i) \sin\phi \sin\theta] \\ &+ \hat{\phi} [(\cos v \cdot \cos\phi_i + \sin v \cdot \cos\theta_i \cdot \sin\phi_i) \sin\phi + (-\cos v \cdot \sin\phi_i \\ &+ \sin v \cdot \cos\theta_i \cdot \cos\phi_i) \cos\phi] \} \end{aligned} \quad (17)$$

where

$$\alpha = \frac{1}{2} kb(\sin\theta_i \cos\phi_i + \sin\theta \cos\phi) \quad (18)$$

$$\beta = \frac{1}{2} kc(\sin\theta_i \sin\phi_i + \sin\theta \sin\phi) \quad (19)$$

and b and c are the dimensions of the conducting plate.

2.5 Field reradiated from the Van Atta reflector and its image.

The electric field reradiated from the dipoles and their images is given by

$$\bar{E}_{\text{reflector}} = \bar{E}_{\text{ref}}(R, \theta, \phi) [G_{\text{dipole}}(\theta, \phi) + G_{\text{image}}(\theta, \phi)] \quad (20)$$

Here

$$\begin{aligned} \bar{E}_{\text{ref}}(R, \theta, \phi) &= \frac{i \zeta_0 E_0 \epsilon^{ikR}}{\pi \cdot Z_0 \cdot kR} \cdot \frac{\cos(\frac{\pi}{2} \sin\theta \sin\phi)}{\sqrt{1 - \sin^2\theta \sin^2\phi}} \\ &[\sin\phi \cos\theta \cdot \hat{\theta} + \cos\phi \cdot \hat{\phi}] \end{aligned} \quad (21)$$

is the reradiated electric field at a point in the distance R from a reference antenna in (0,0,0), and

$$G_{\text{dipole}}(\theta, \phi) \quad \text{and} \quad G_{\text{image}}(\theta, \phi)$$

are the array factors in the plane of dipoles and in the plane of image-dipoles, respectively.

The array factors may be expressed as

$$G(\theta, \phi) = \sum_{n=1}^N i_n \cdot e^{-ik\vec{r}_n \cdot \hat{f}} \quad (22)$$

where N is the number of antenna elements in the array, i_n is the complex current induced in the n 'th dipole, \vec{r}_n is the radiusvector from the point of reference $(0,0,0)$ to the n 'th antenna, and \hat{f} is a unit vector in the direction from $(0,0,0)$ to the field point.

Introducing the unit vector

$$\hat{f} = \hat{x} \cdot \sin\theta \cos\phi + \hat{y} \cdot \sin\theta \sin\phi + \hat{z} \cdot \cos\theta \quad (23)$$

and the radiusvectors of the n 'th dipole and the n 'th image dipole:

$$\begin{aligned} \vec{r}_{n,\text{dipole}} &= (x_n, y_n, 0) \\ \vec{r}_{n,\text{image}} &= (x_n, y_n, -2h) \end{aligned}$$

and remembering that the currents of the image dipoles are equal to and with opposite sign of the currents of the real dipoles we find

$$\vec{E}_{\text{reflector}} = \vec{E}_{\text{ref}}(R, \theta, \phi) G_{\text{reflector}}(\theta, \phi) \quad (24)$$

where

$$\begin{aligned} G_{\text{reflector}}(\theta, \phi) &= G_{\text{dipole}}(\theta, \phi) + G_{\text{image}}(\theta, \phi) \\ &= \sum_{n=1}^N i_n \{ e^{-ik(x_n \sin\theta \cos\phi + y_n \sin\theta \sin\phi)} \\ &\quad - e^{-ik(x_n \sin\theta \cos\phi + y_n \sin\theta \sin\phi - 2h \cos\theta)} \} \quad (25) \end{aligned}$$

2.6 Total reradiated field.

The total electric field \vec{E}_{total} reradiated from the reflector system con-

sisting of the simple Van Atta reflector and the conducting plate, may be found by adding the electric field reflected from the plate \vec{E}_{plate} (Eq. 17) and the electric field reradiated from the Van Atta reflector and its image $\vec{E}_{\text{reflector}}$ (Eq. 24):

$$\vec{E}_{\text{total}}(R, \theta, \phi) = \vec{E}_{\text{plate}}(R, \theta, \phi) + \vec{E}_{\text{reflector}}(R, \theta, \phi) \quad (26)$$

3. NUMERICAL INVESTIGATION

3.1 Description of the properties of the reflector.

When describing reradiation or scattering properties the most commonly used quantity is the differential scattering cross section, which in an arbitrary direction and independent of the distance gives the far field scattered from a target for an incident plane wave. The scattering cross section in the direction opposite to the direction of incidence of the plane wave is called the back-scattering cross section.

The differential scattering cross section is defined by

$$\sigma(\theta, \phi) = 4\pi R^2 \frac{|\vec{S}_r(\theta, \phi) \cdot \hat{n}_r|}{|\vec{S}_i(\theta, \phi) \cdot \hat{n}_i|} \quad (27)$$

where \vec{S}_r and \vec{S}_i are the Poynting vectors of the reflected and incident fields, and \hat{n}_r and \hat{n}_i are unit vectors in the direction of propagation of the reflected and incident fields, respectively.

For the incident plane wave we have

$$|\vec{S}_i \cdot \hat{n}_i| = \frac{1}{2} \frac{E_o^2}{\zeta_o} \quad , \quad (28)$$

and for the wave reradiated from the Van Atta reflector with the conducting plate from equation (26)

$$|\vec{S}_r \cdot \hat{n}_r| = \frac{1}{2} \frac{|\vec{E}_{total}|^2}{\zeta_o} \quad (29)$$

In the numerical investigations discussed in the next sections the electric field reradiated from the Van Atta reflector with or without the conducting plate will be described by the normalized scattering cross section $\sigma(\theta, \phi)/\lambda^2$. Especially the back-scattering cross section σ_b/λ^2 of the reflector will be discussed.

3.2 Comparison with results obtained by Sharp.

As mentioned previously Sharp⁶⁾ has made an experimental investigation of a square Van Atta reflector consisting of 16 half-wave dipoles mounted parallel to and a quarter of a wavelength above a conducting plate. The dipoles were set up in a four-by-four array with a spacing of 0.6 wavelengths. The frequency used was 2850 Mc/s corresponding to a wavelength $\lambda = 10.519$ cm. The interconnecting transmission lines were of the length 22.5 ± 0.1 inches which corresponds to the electrical length $5.433\lambda \pm 0.024\lambda$.

The comparison between this experimental reflector and the Van Atta reflector investigated here is carried out by considering the back-scattering cross section σ_b/λ^2 of the reflectors in the xz-plane ($\phi_i = 0^\circ$), when the incident plane wave is polarized parallel to the dipoles. From the report made by Sharp⁶⁾ the curve denoted "array" in pattern 1 is redrawn in fig. 4 of this report. In the same figure the computed values of σ_b/λ^2 is shown for a reflector with the same parameters as Sharp's model. In order to obtain matching conditions between the dipoles and the transmission lines the characteristic impedance of the lines is $Z_0 = 73$ ohms.

Because of the uncertainty in the actual electrical length of the transmission lines of the experimental reflector, a number of reflectors with various lengths of the lines has been examined theoretically. It turned out that transmission lines of the length $a = 0.41\lambda$ gave the reradiation pattern which was closest to the one measured by Sharp. This value is in accordance with the value given for the experimental reflector ($0.43\lambda \pm 0.02\lambda$).

From the two curves in fig. 4 it is seen that, for angles of incidence θ_i less than 60° , the back-scattering cross section of the experimental and theoretical reflector differ with an amount of at most 2.6 db. When θ_i is larger than 60° the edge of the conducting plate will influence the reradiated field to such a degree that a comparison between the measured and computed results would not be reasonable.

Probably, the discrepancies between the two curves of fig. 4 to some extent are due to inaccuracies in the experiments. The curves denoted "flat plate" in pattern 1 and pattern 2 of Sharp's report show the measured values of σ_b/λ^2 for the same square, conducting plate obtained during two different measurements. It is seen that the two curves for θ_i less than 60° deviates with about 2.0 - 2.5 db, and that there is an angular displacement of the curves of about $3^\circ - 9^\circ$. This shows the uncertainty of the measurements and it is seen that the theoretical and experimental curves of fig. 4 agree within the limits of this uncertainty for angles of incidence less than 60° .

In fig. 5 is shown the experimental and theoretical values of σ_p/λ^2 for the conducting plate itself.

The size of the square conducting plate is $N \cdot d^2$, where N is the number of dipoles and d the distance between adjacent dipoles. A plate of this size covers the whole area below the dipoles. For the 16 element Van Atta reflector considered in this section the size of the plate is $5.76\lambda^2$ in accordance with the size of the plate in Sharp's model.

From fig. 5 it turns out that there is a good agreement between the two curves when the angle of incidence θ_i is less than 60° , so that the edges of the plate do not affect the reradiated field.

A better agreement for θ_i larger than 60° may be obtained if the diffraction of the field about the edges of the plate is taken into account. These diffractive effects might probably be introduced into the calculations if the field reflected from the plate was determined by means of the geometrical theory of diffraction instead of the physical optics method used here ¹⁰⁾.

3.3 Effect of changing the parameter values.

The parameters of the reflector are:

- N: the number of elements,
- d: the distance between adjacent elements,
- h: the distance between the elements and the plate,
- Z_0 : the characteristic impedance of the transmission lines, and
- a: the length of the transmission lines.

In this section we will investigate what happens to the back-scattering cross section σ_p/λ^2 of the reflector when these parameters are varied in turn. The incident field is polarized parallel to the dipoles and $\phi_i = 0^\circ$. As a starting point for the variations we choose the reflector which was compared with Sharp's experimental model in section 3.2.

The initial values of the parameters will then be $N = 16$ elements, $d = 0.6\lambda$, $h = 0.25\lambda$, $Z_0 = 73$ ohms, and $a = 0.41\lambda$. We will consider both the simple reflector and the reflector with the conducting plate except in the case where the distance h between the elements and the plate is varied.

In fig. 6 is shown how σ_p/λ^2 changes when the number of dipole elements in the reflector is increased from two-by-two up to six-by-six elements. As expected the reradiated energy is increased when the number of elements increases and both in the case with and without the conducting plate the total increment is about 30 db for normal incidence ($\theta_i = 0^\circ$). Furthermore, it turns out that the

curves become more irregular the more elements the reflector consists of and that the presence of the conducting plate makes the values of σ_b/λ^2 decrease more quickly when the angle of incidence θ_i increases towards 90° .

In fig. 7 the distance between adjacent dipoles is varied from $d = 0.6\lambda$ to $d = 1.5\lambda$. It will be noticed that σ_b/λ^2 in the direction normal to the reflector ($\theta_i = 0^\circ$) has a minimum when $d = 1.0\lambda$. This minimum is most pronounced when the conducting plate is taken into account, but occurs in the case of the simple reflector, too. When d increases it appears that the irregularities of the curve of σ_b/λ^2 increase but it also turns out that the level of back-scattering for θ_i larger than 40° is increased essentially. Since the coupling between the dipoles decreases for increasing d , the latter is in agreement with the fact that coupling usually makes the minimum value of σ_b/λ^2 decrease. This is shown in SR4 for a linear four-element Van Atta reflector.

Changing the distance h from the dipoles to the conducting plate from $h = 0.05\lambda$ to $h = 0.5\lambda$ results in the curve of σ_b/λ^2 shown in fig. 8. It is seen that the back-scattering in the direction $\theta_i = 0^\circ$ obtains its smallest value when $h = 0.25\lambda$, which is the distance Sharp used in his experimental model. From fig. 8 it appears that a higher level of back-scattering for all angles of incidence might have been obtained by choosing $h = 0.35\lambda$ in the experimental model instead of $h = 0.25\lambda$.

The characteristic impedance of the transmission lines is varied from $Z_0 = 15$ ohms to $Z_0 = 150$ ohms and the results are shown in fig. 9. When the plate is not taken into account it turns out that σ_b/λ^2 increases for $0^\circ < \theta_i < 45^\circ$, decreases for $45^\circ < \theta_i < 70^\circ$ and again increases for $\theta_i > 70^\circ$ when the characteristic impedance Z_0 is increased up to 150 ohms. For θ_i equal to 0° , 45° , and 70° the value of σ_b/λ^2 is almost unchanged. When the conducting plate is taken into account the same occurs except for the range $70^\circ < \theta_i < 80^\circ$ where σ_b/λ^2 now is practically unchanged. It is seen that the curve of σ_b/λ^2 in this way obtains a more smooth shape for larger values of Z_0 , especially when the plate is taken into account. Unfortunately σ_b/λ^2 decreases much faster for increasing θ_i at the same time.

In fig. 10 the length of the transmission lines is varied from $a = 0.0\lambda + p\lambda$ to $a = 1.0\lambda + p\lambda$ where p is an integer. When the plate is not taken into account it turns out that σ_b/λ^2 in the direction normal to the reflector tends to zero when $a = p\lambda$ whereas it has a maximum for $a = 0.5\lambda + p\lambda$. Furthermore, the curve has a deep minimum in the direction $\theta_i = 57^\circ$ when $a = 0.5\lambda + p\lambda$. When the conducting plate is taken into account the minimum of σ_b/λ^2 for $a = p\lambda$ in the normal direction is changed to a maximum whereas the maximum for $a = 0.5\lambda + p\lambda$

is unchanged. Further two new minima occur for $a = 0.1\lambda + p\lambda$ and $a = 0.9\lambda + p\lambda$, respectively and the deep minimum in the direction $\theta_i = 57^\circ$ when $a = 0.5\lambda + p\lambda$ is essentially reduced. It is seen that the length of the lines chosen by Sharp in his experimental investigation, which is $a = 0.43\lambda$ (5.43λ), appears to be almost the best possible choice if maximum of σ_b/λ^2 in the normal direction and a smooth shape of the curve is wanted.

3.4 Effect of turning the plane of incidence.

The plane of incidence is turned by gradually changing ϕ_i from 0° to 90° . The incident plane wave is polarized in a direction parallel to the plane of the dipoles and perpendicular to the plane of incidence. In fig. 11 and fig. 12 the back-scattering cross section is plotted in polar coordinates for a Van Atta reflector with and without the conducting plate, respectively. The reflector has the same parameters as the basic reflector of the preceding section.

From fig. 11 it appears that the shape of the curve of σ_b/λ^2 becomes more smooth when ϕ_i is increased from 0° to 80° , but at the same time the level of back-scattered energy decreases and for $\phi_i = 90^\circ$ no energy at all is reradiated from the reflector since the incident wave is then polarized perpendicular to the dipoles.

From fig. 12, where the presence of the conducting plate is taken into account, it is seen, too, that the shape of the curves becomes more smooth when ϕ_i is increased, but because of the plate the level of back-scattered energy is not decreasing so much, and for $\phi_i = 90^\circ$ all the back-scattered energy is due to the plate.

In order to obtain a measure of the angular coverage of the reflector, the curves in fig. 13 have been drawn. They show the angle over which the back-scattering cross section decreases 3 db (respectively 5 db) below the maximum value. This angle is called the 3 db-response angle (respectively 5 db-response angle). From the curves it appears, that the Van Atta reflector with the conducting plate shows a larger response angle than the reflector without plate over an angular range from $\phi_i = 0^\circ$ to $\phi_i = 50^\circ$. Although the calculated response angles show fluctuations as a function of ϕ_i it can be stated that the average 5 db-response angle of the reflector with the conducting plate is almost twice as large as that of the dipole reflector alone in the angular range between $\phi_i = 0^\circ$ and $\phi_i = 45^\circ$. For the 3 db-response angle this angular range is between $\phi_i = 0^\circ$ and $\phi_i = 30^\circ$.

4. CONCLUSION

Arbitrary Van Atta reflectors with or without a conducting plate has been investigated analytically and numerically. When the plate is not taken into account, the reflector is investigated as described in SRL.

If the plate is present the reflecting system consists of two devices, the dipoles and the plate. The system of dipoles is then treated along the same lines as in SRL, but the presence of the plate will influence the dipole system in such a way that the induced voltage, the mutual impedances, and the determination of the reradiated field have to be changed. The reflecting properties of the plate are supposed not to be affected by the shadowing-effect of the dipoles.

The numerical investigation, which has been made on an IBM 7090 electronic computer, shows a good agreement with the experimental reflector investigated by Sharp ⁶⁾. The effect of varying the parameters of the reflector has been investigated by considering the back-scattering cross section of several different reflectors with or without the conducting plate. From an examination of the results obtained it turns out that the presence of a conducting plate in a distance h below the dipole system will cause both advantages and disadvantages. Among the first the most pronounced is a rise of the level of back-scattering in the direction normal to the plane of the reflector and a highly increased 5 db-response angle, while the largest disadvantage is that the back-scattering cross section is decreasing very fast when the direction of incidence makes an angle θ_i larger than 60° with the normal to the reflector. Further it turns out that by choosing proper values of the parameters the reradiation pattern may be changed to compare better with a prescribed form and that the values of the parameters used in Sharps experimental model are not the best possible in order to obtain a Van Atta reflector that behaves as stated in the patent description.

5. REFERENCES

1. Tove Larsen, "A theoretical investigation of Van Atta arrays". Scientific Report No. 1, Contract No. Af 61(052)-794, Laboratory of Electromagnetic Theory, Technical University of Denmark, Nov. 1964.
2. J. Appel-Hansen, "Linear Van Atta reflector consisting of four half-wave dipoles". Scientific Report No. 2, Contract No. AF 61(052)-794, Laboratory of Electromagnetic Theory, Technical University of Denmark, Nov. 1964.
3. J. Appel-Hansen, "Experimental investigation of a linear Van Atta reflector". Scientific Report No. 3, Contract No. AF 61(052)-794, Laboratory of Electromagnetic Theory, Technical University of Denmark, May 1965.
4. J. Appel-Hansen, "Optimization of the reradiation pattern of a Van Atta reflector". Scientific Report No. 4, Contract AF 61(052)-794, Laboratory of Electromagnetic Theory, Technical University of Denmark, July 1966.
5. Tove Larsen, "Reflector arrays". Annual Summary Report, Contract No. AF 61(052)-794, Laboratory of Electromagnetic Theory, Technical University of Denmark, April 1965.
6. E.D. Sharp, "Properties of the Van Atta reflector array". Rome Air Dev. Center technical report 58-53. AD 148684, April 1958.
7. J.A. Fusca, "Compact reflector has c.c.m. potential". Aviation Week, p 66-69, January 5, 1959.
8. E.D. Sharp and M.B. Diab, "Van Atta reflector array". IRE Trans. on Antennas and Propagation, Vol. AP-8, pp 436-438, 1960.
9. D.E. Kerr, "Propagation of short radio waves". M.I.T. Rad. Lab. Ser., Vol. 13 p 456. McGrawHill 1951.
10. R.A. Ross, "Radar cross section of rectangular flat plates as a function of aspect angle". IEEE Trans. on Antennas and Propagation, Vol. AP-14, No. 3, pp 329-335, May 1966.

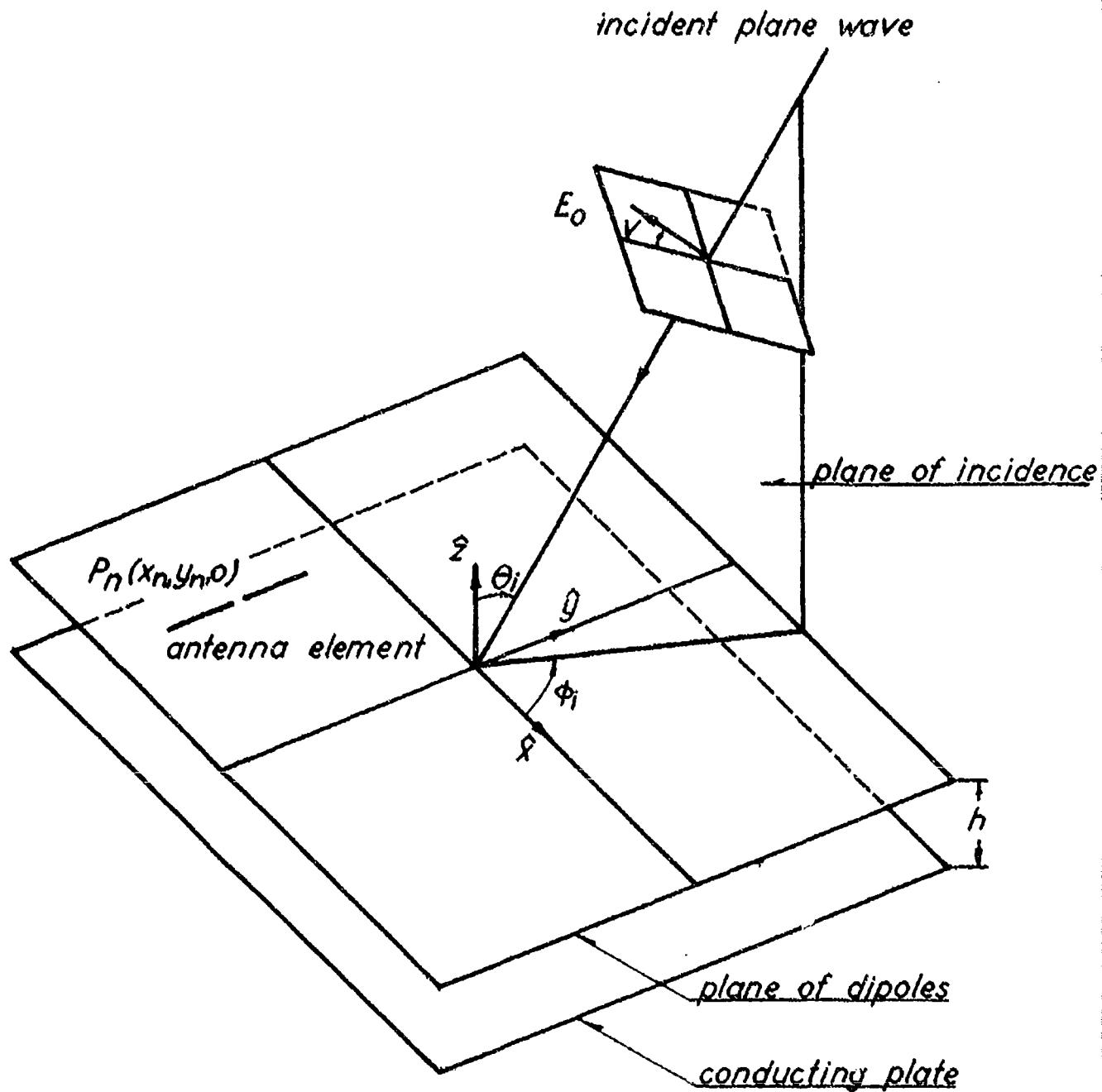


Fig.1. Dipole reflector with conducting plate.

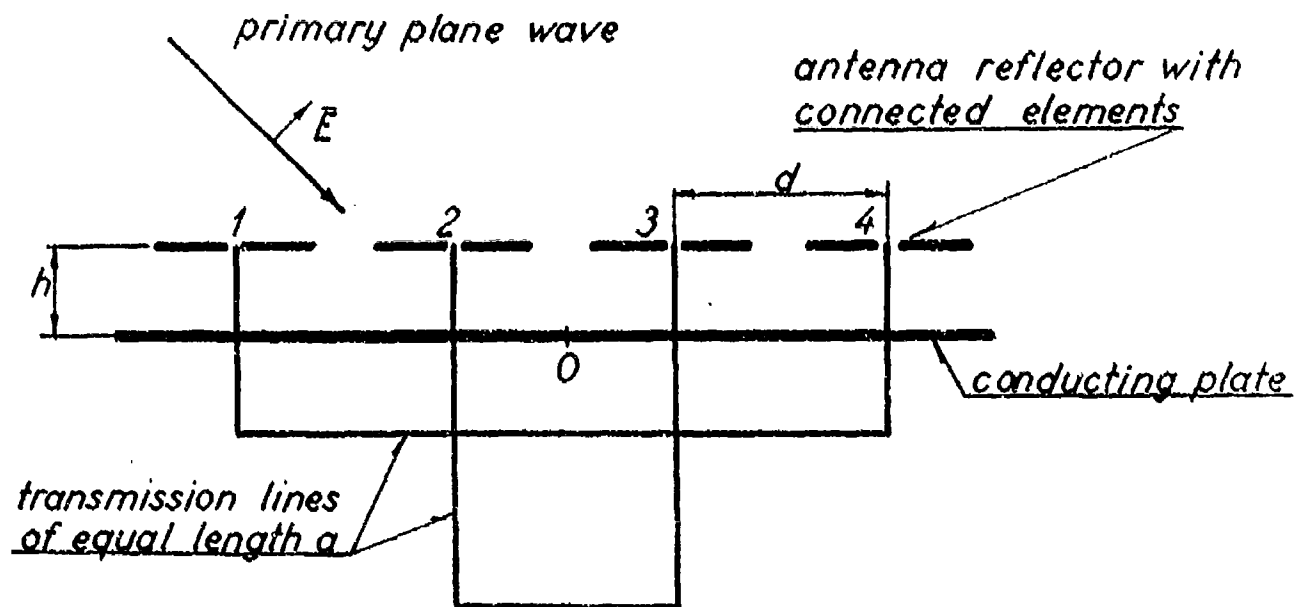


Fig.2a. Configuration investigated.

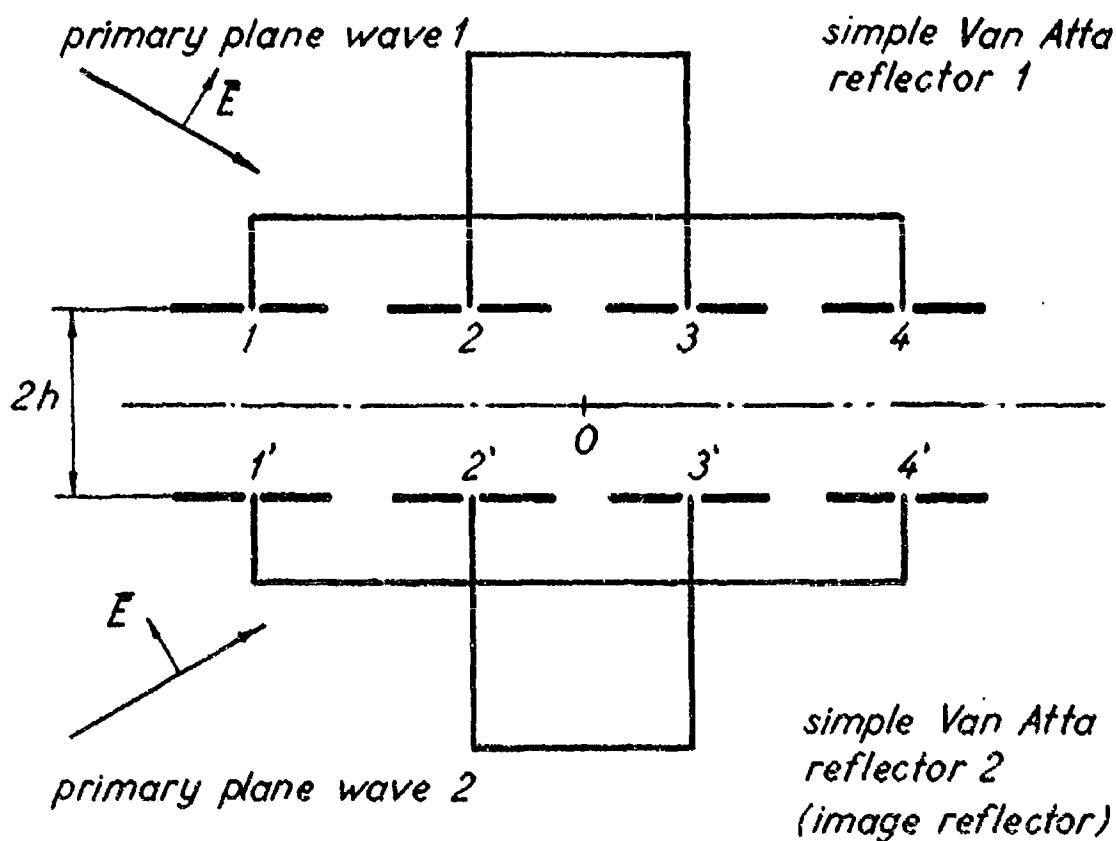


Fig.2b. Using the theory of image.

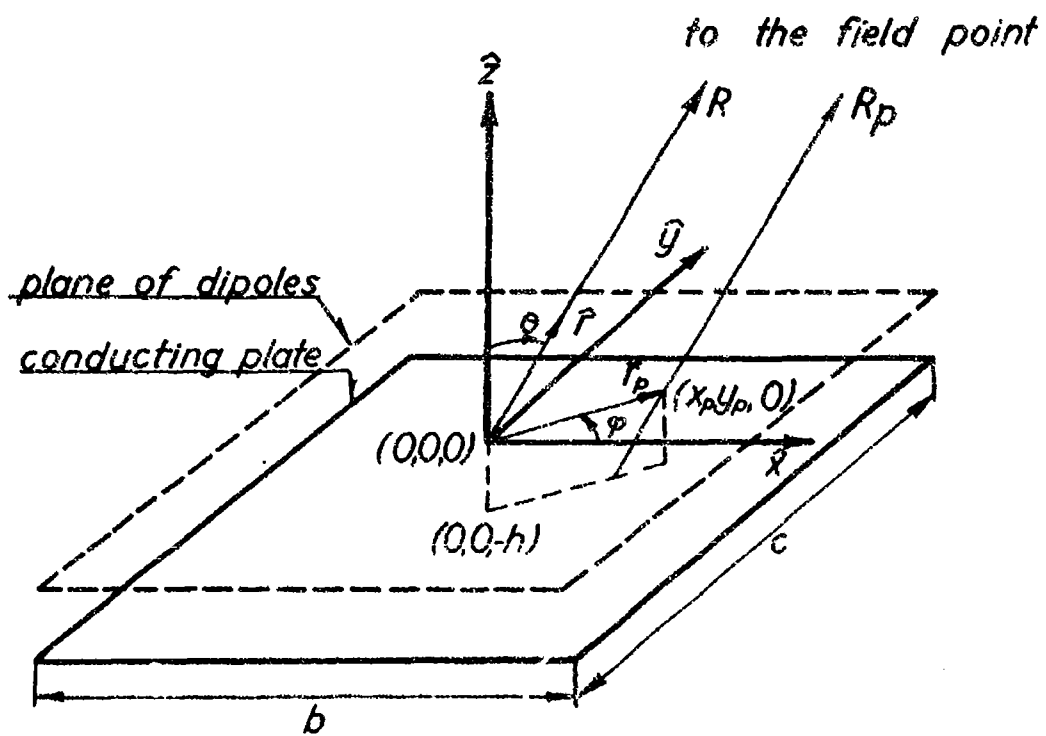


Fig.3 Reradiation from conducting plate.

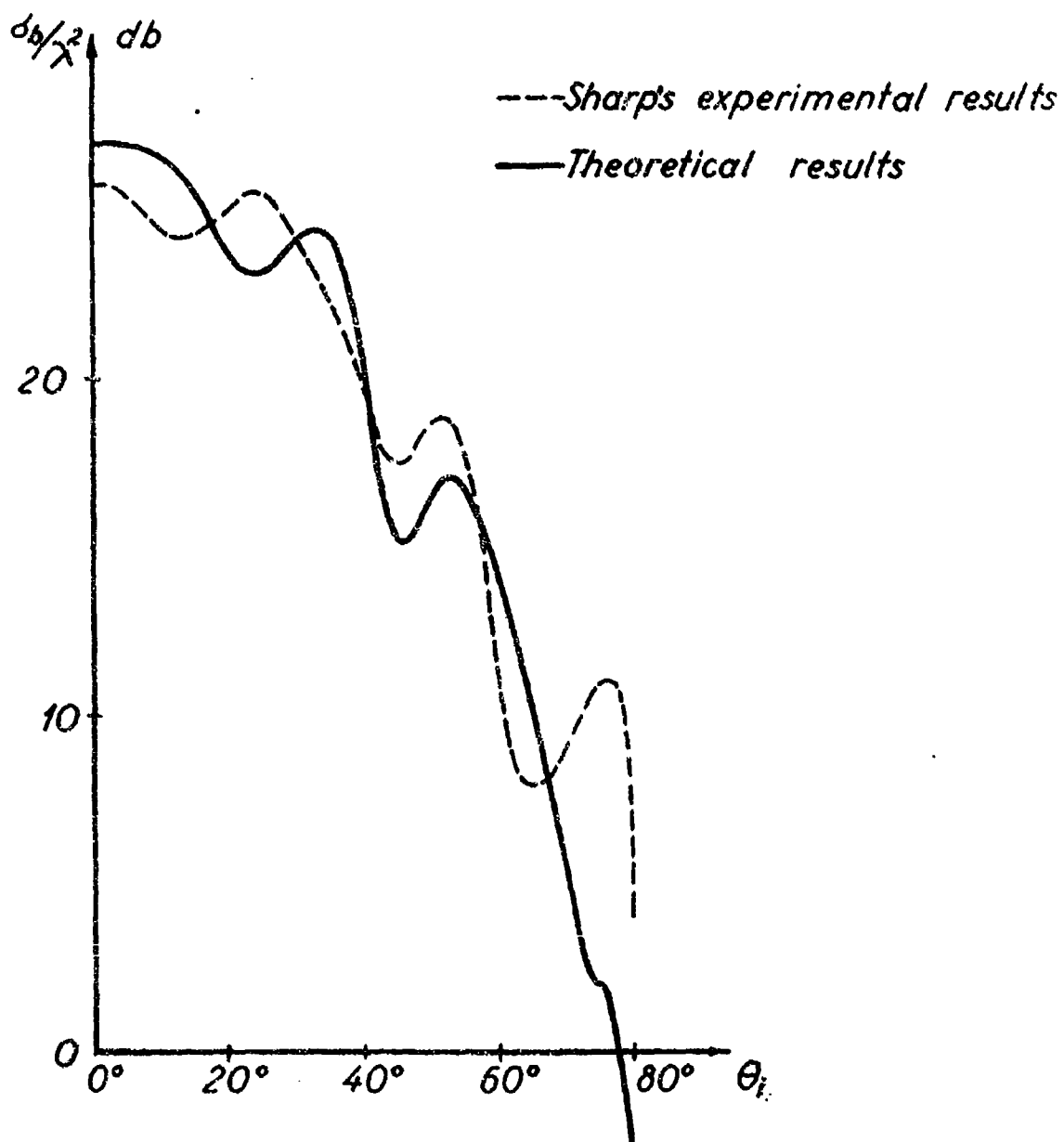


Fig. 4. Normalized back-scattering cross section of 16 element square Van Atta reflector with conducting plate.

$$a = 0.41 \lambda, d = 0.6 \lambda, h = 0.25 \lambda, Z_0 = 73 \text{ ohms},$$

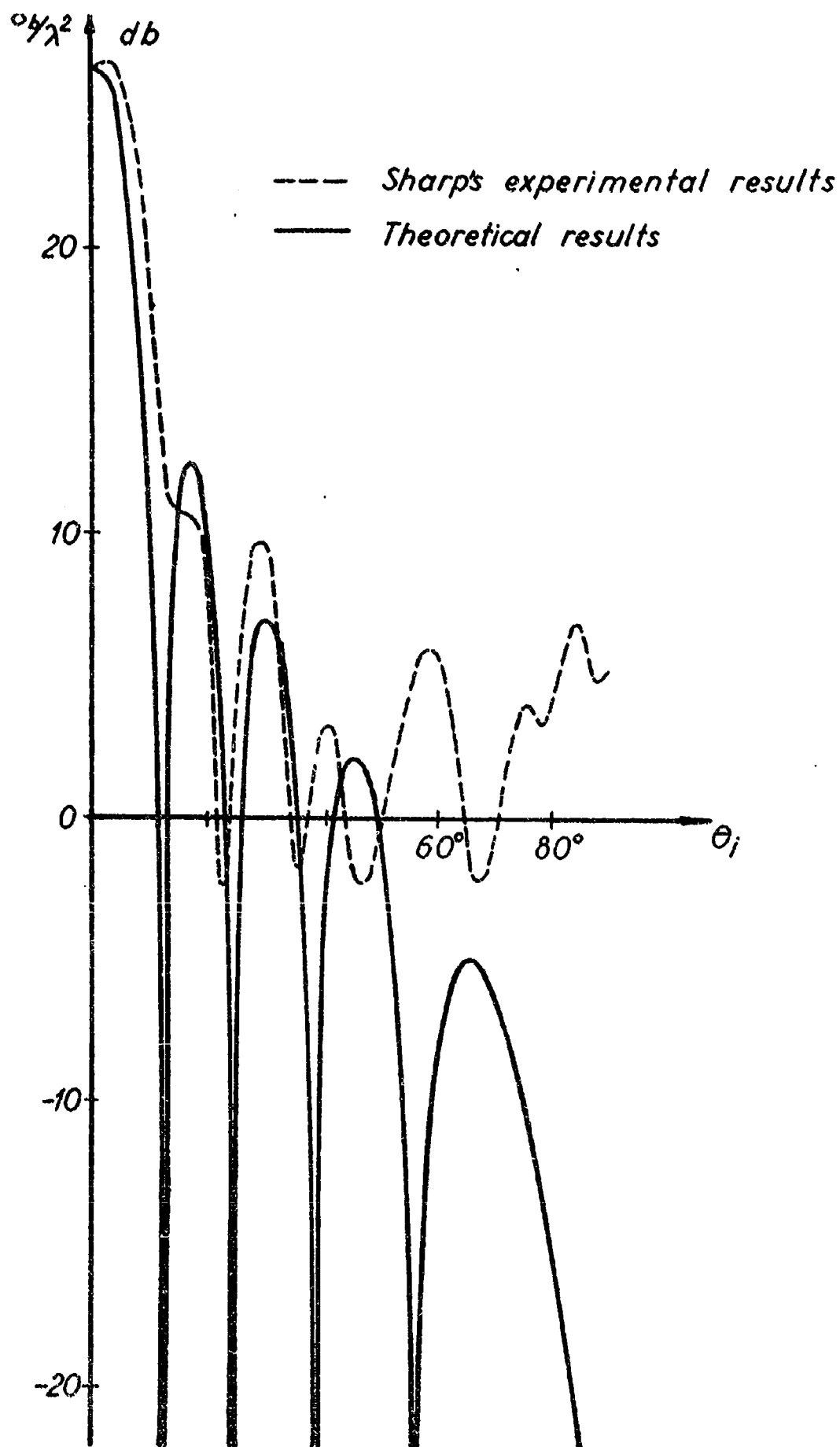


Fig.5. Normalized back-scattering cross section of conducting

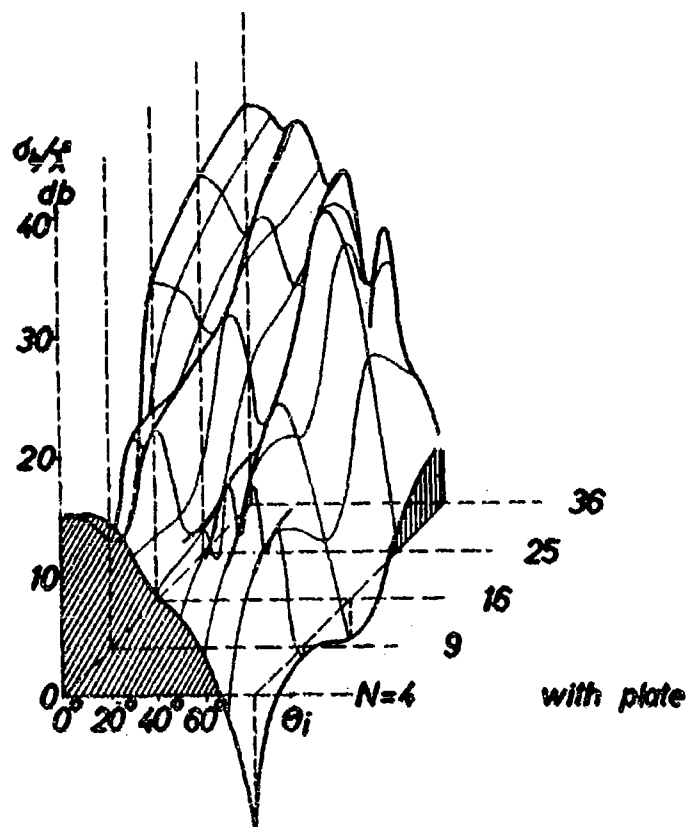
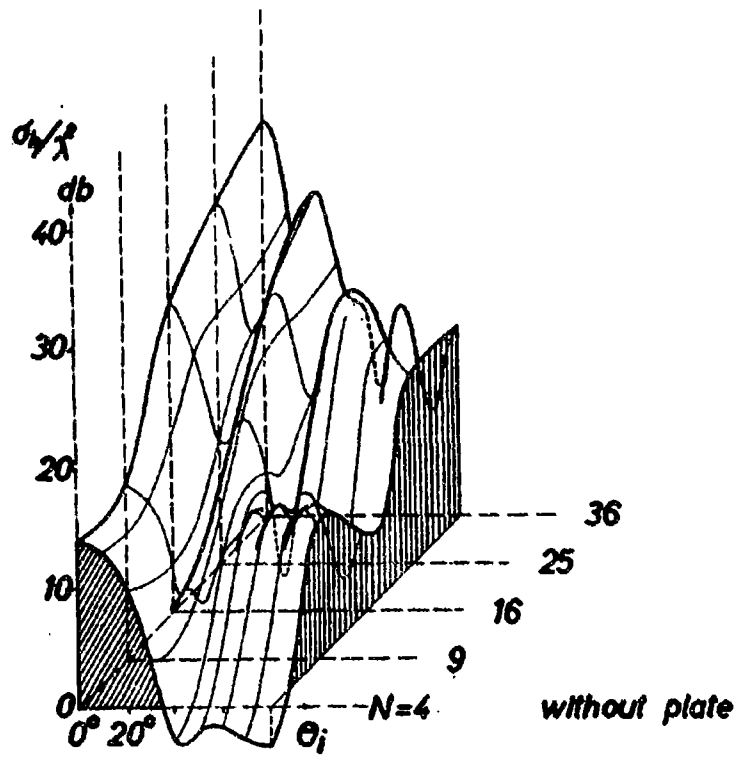


Fig. 6. Normalized back-scattering cross section as a function of the number of dipole elements N .

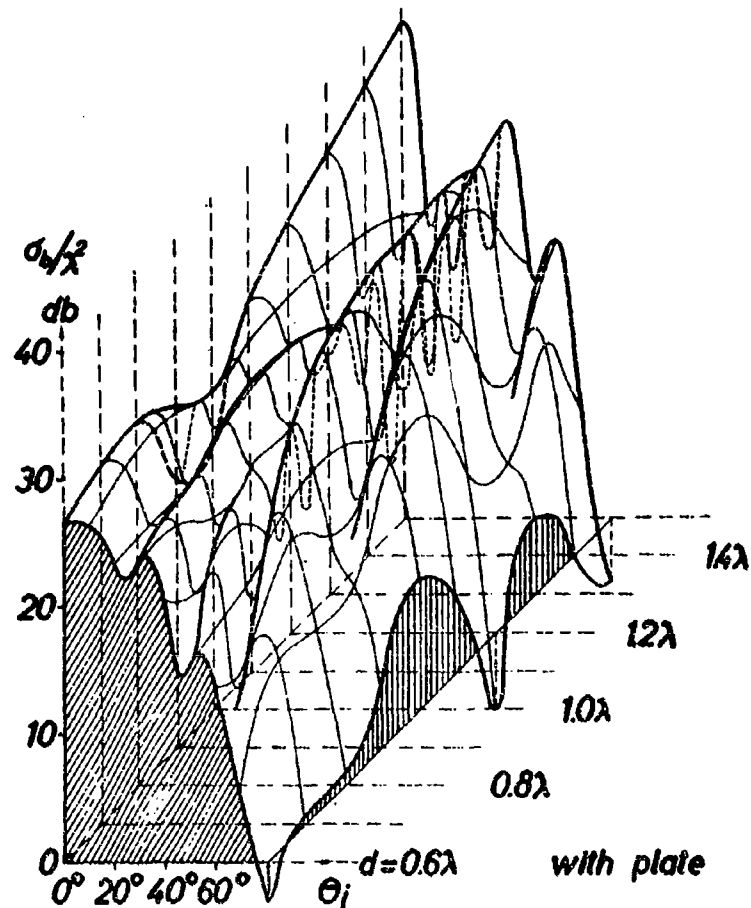
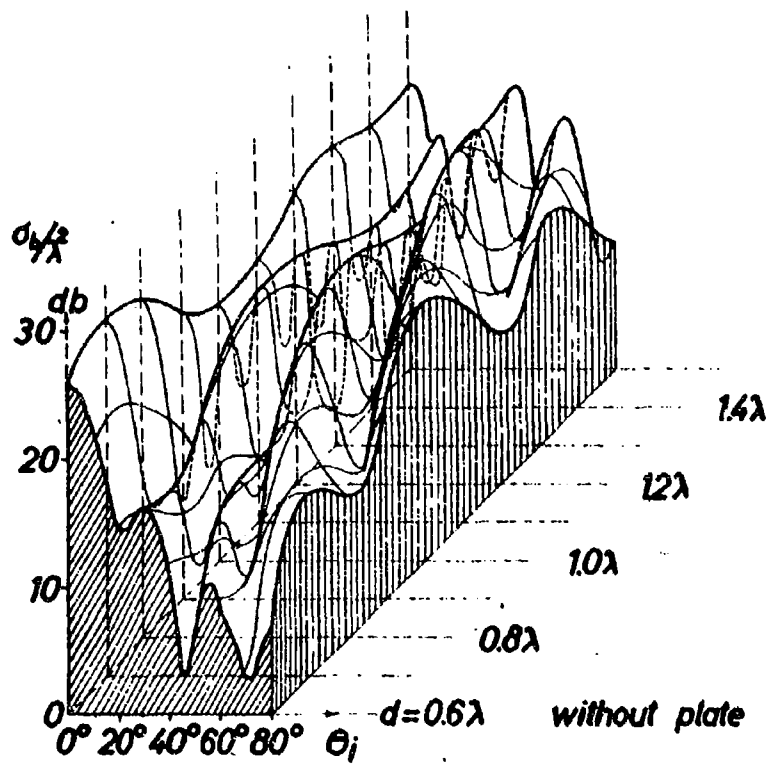


Fig. 7. Normalized back-scattering cross section as a function of the distance d between the dipoles.

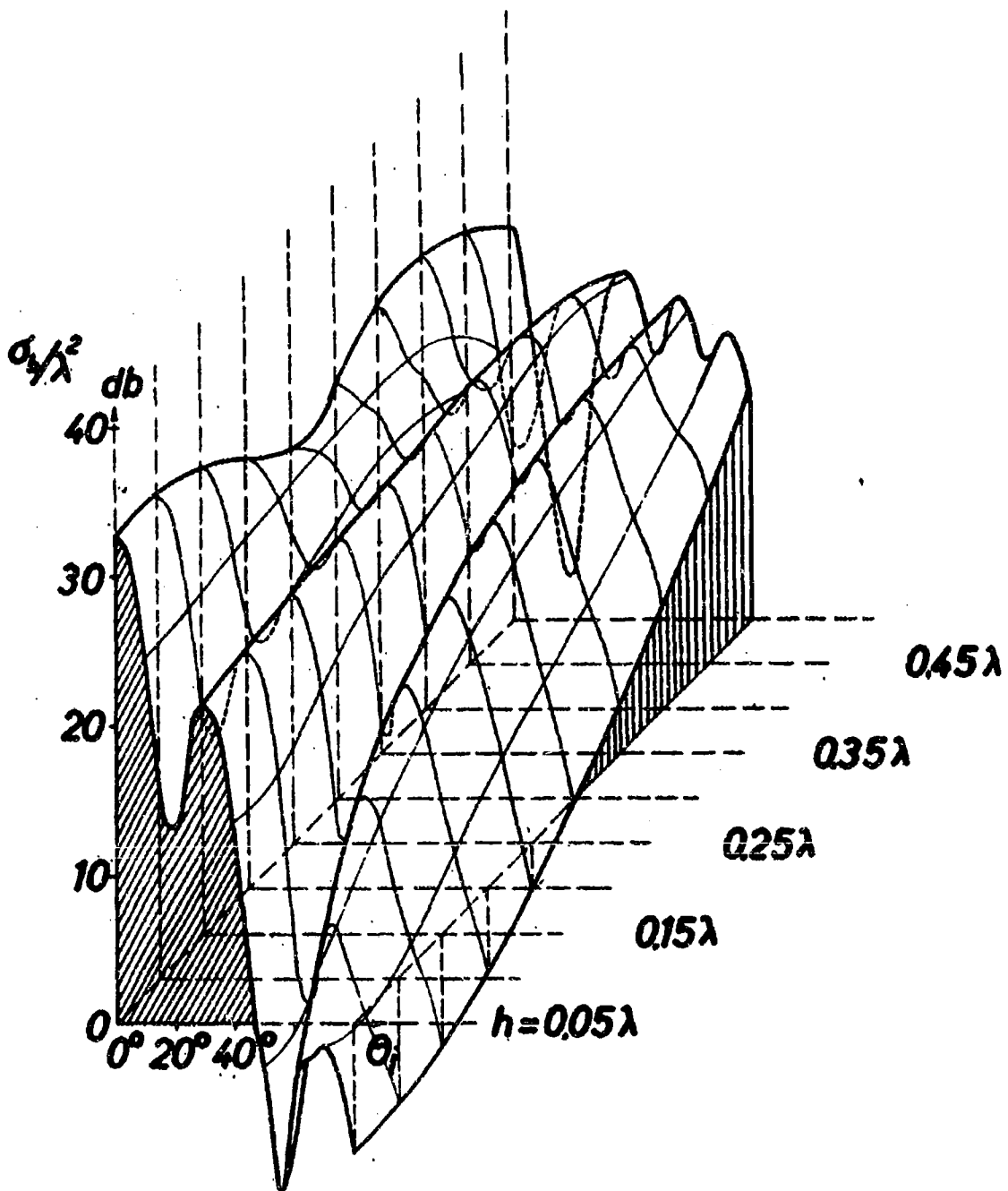


Fig. 8. Normalized back-scattering cross section as a function of the distance h between the dipoles and the plate.
 $N = 16$ elements, $d = 0.6\lambda$, $a = 0.41\lambda$, $Z_0 = 73$ ohms.

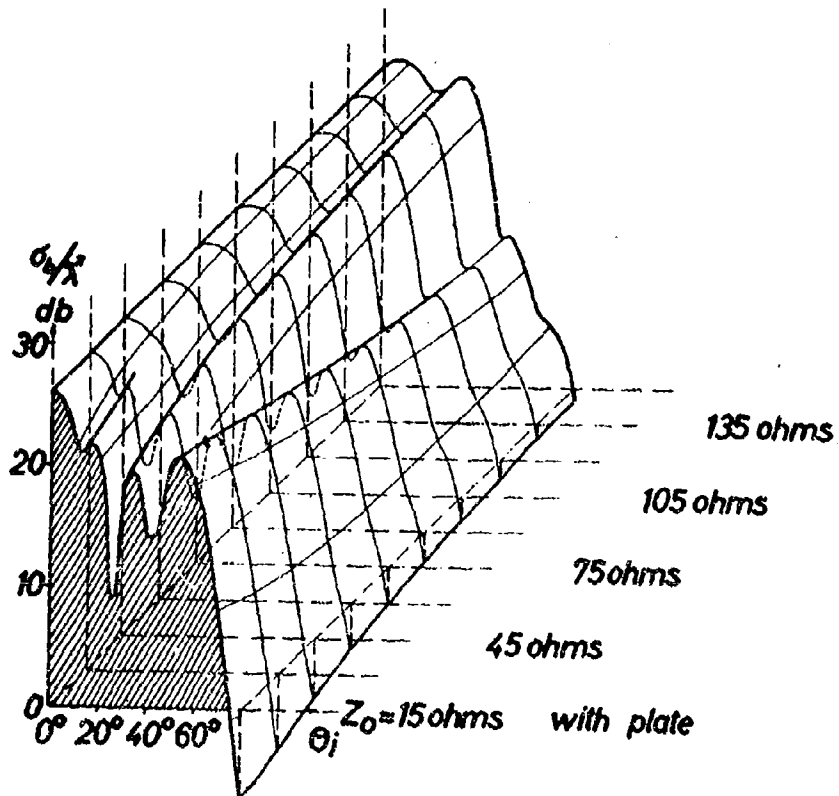
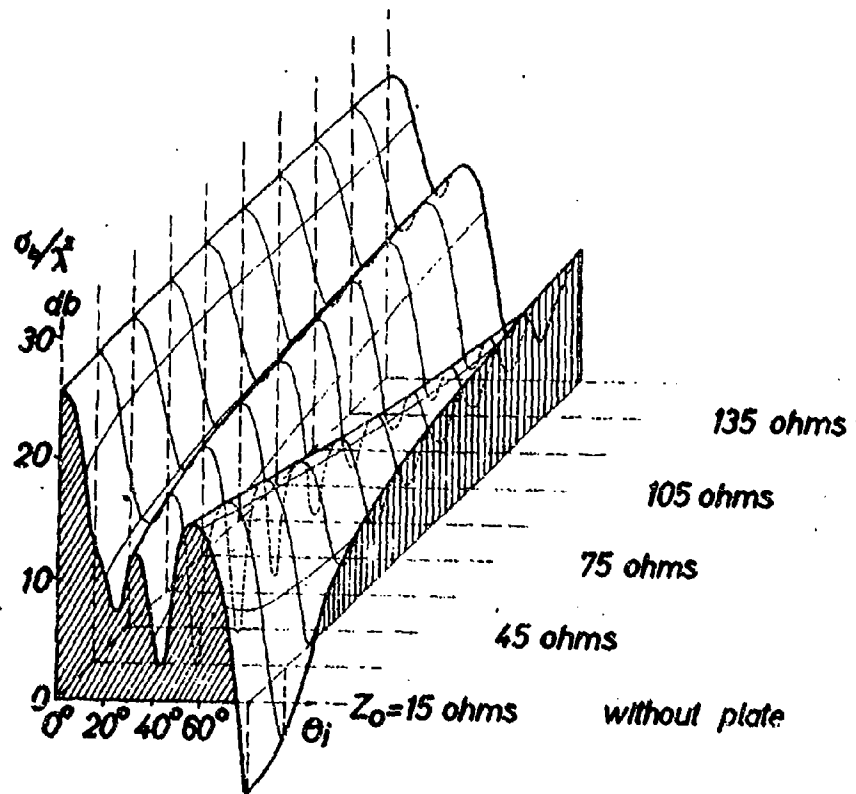


Fig. 9. Normalized back-scattering cross section as a function of the characteristic impedance Z_0 of the transmission lines.

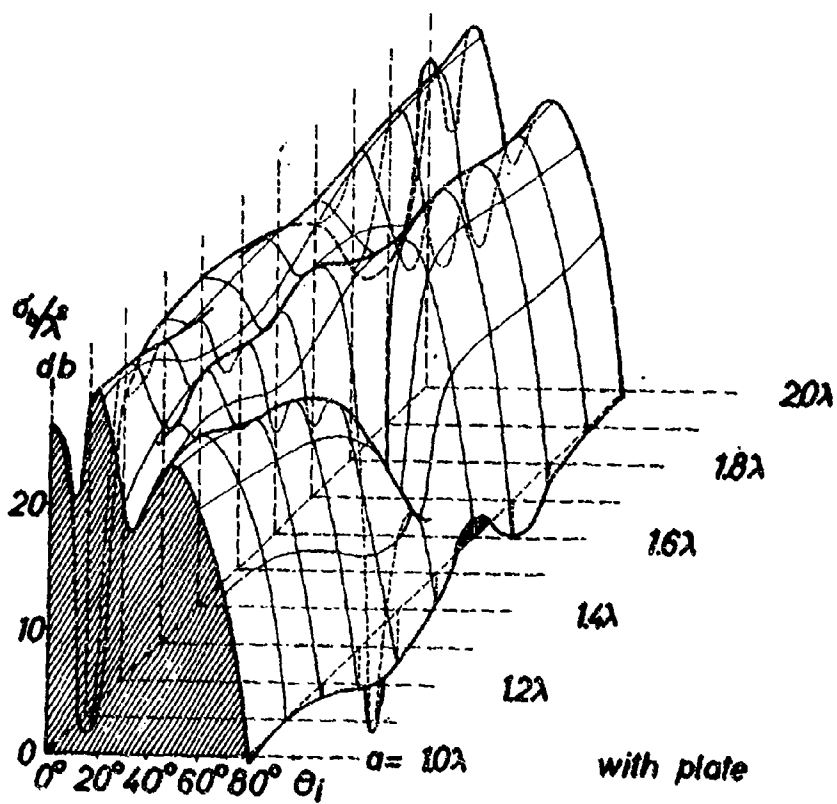
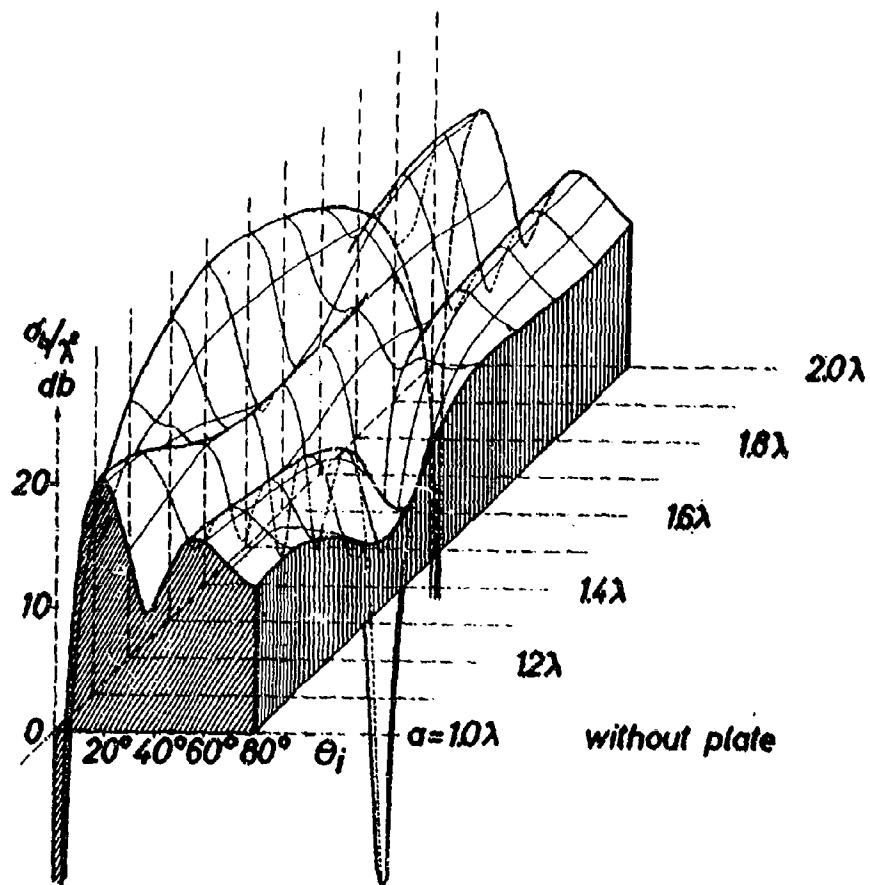


Fig. 10. Normalized back-scattering cross section as a function of the length a of the transmission lines.

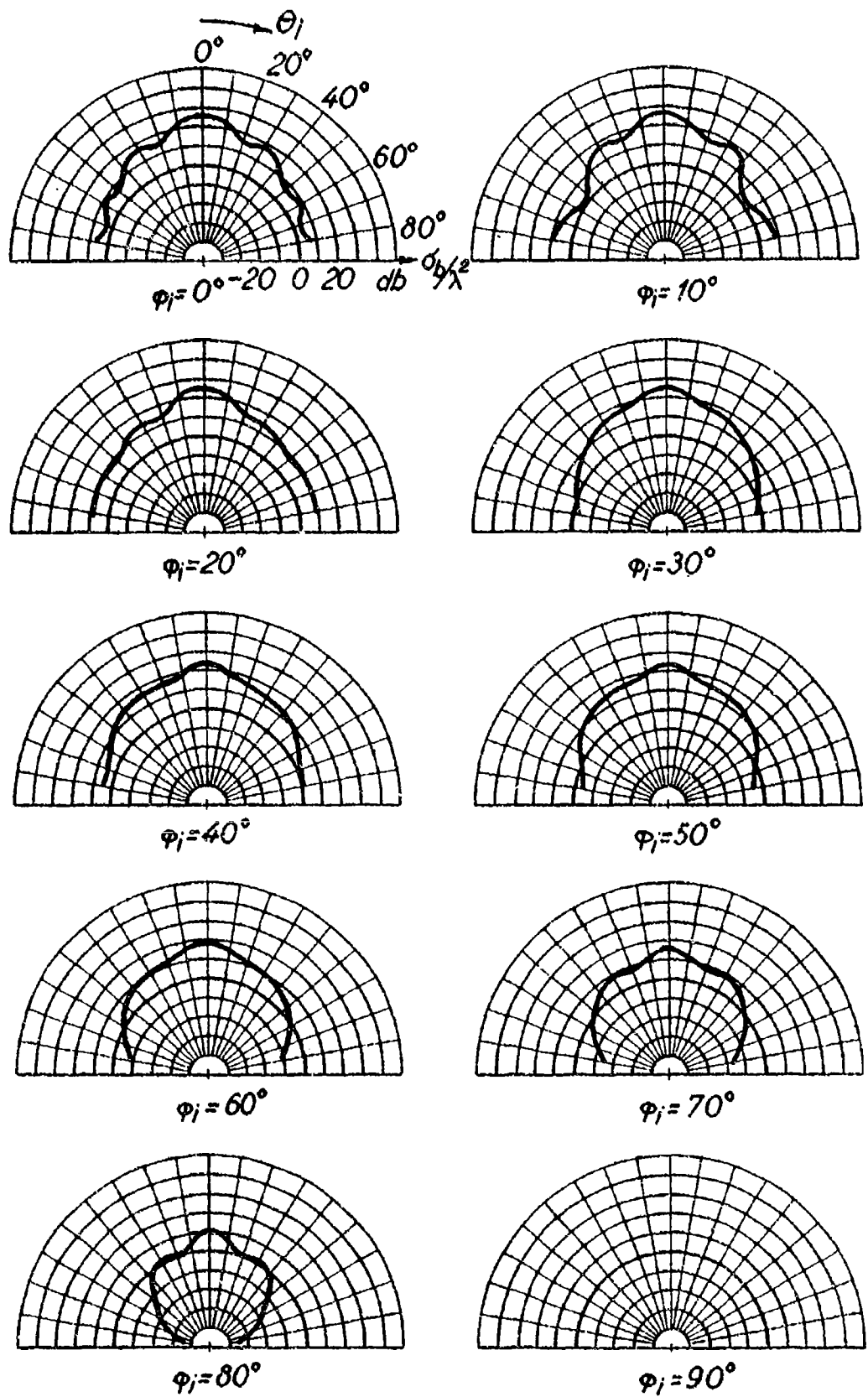


Fig.11 Normalized back-scattering cross section as a function of the angle of incidence θ_j for various values of the

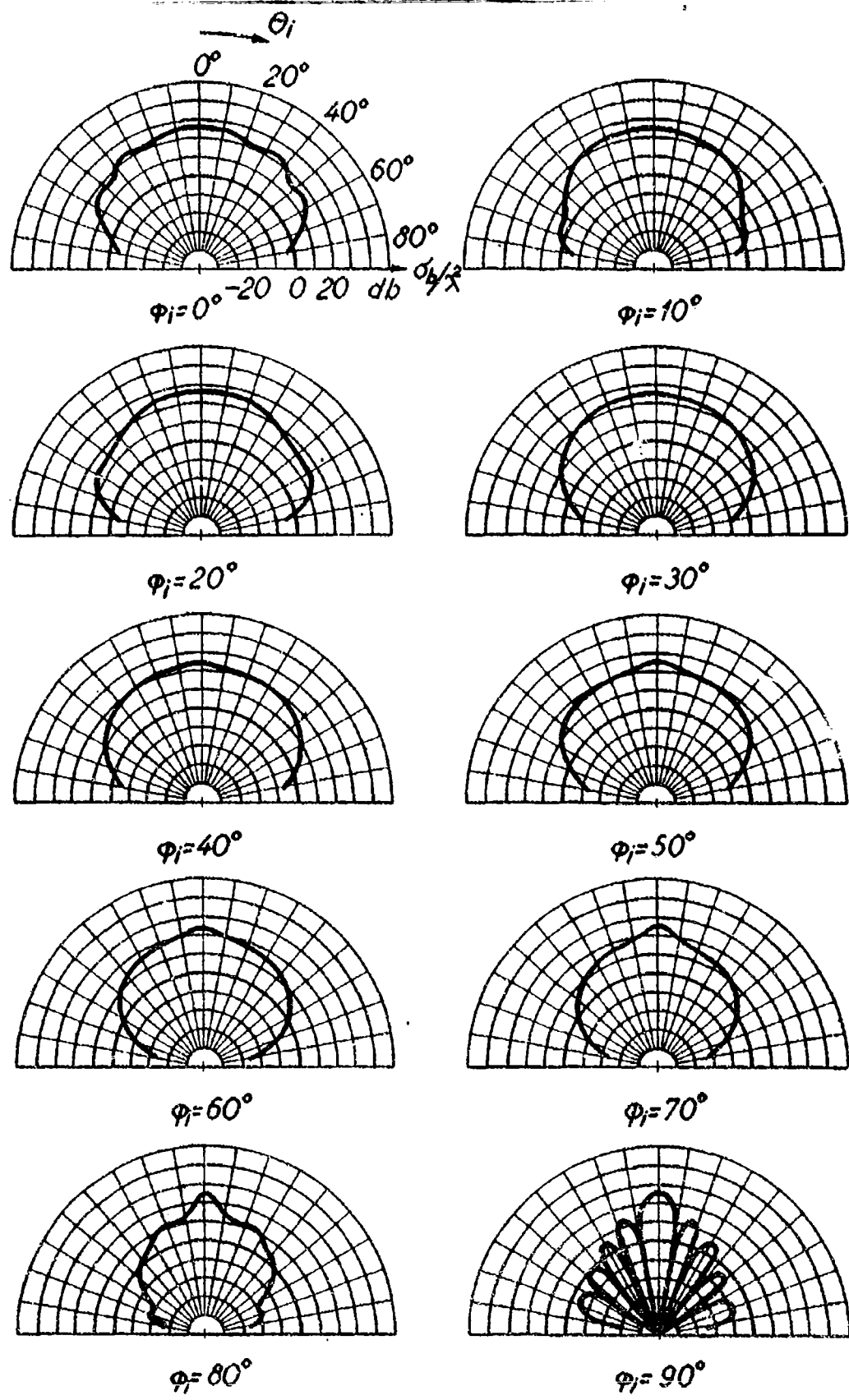


Fig.12. Normalized back-scattering cross section as a function of the angle of incidence θ_i for various values of the

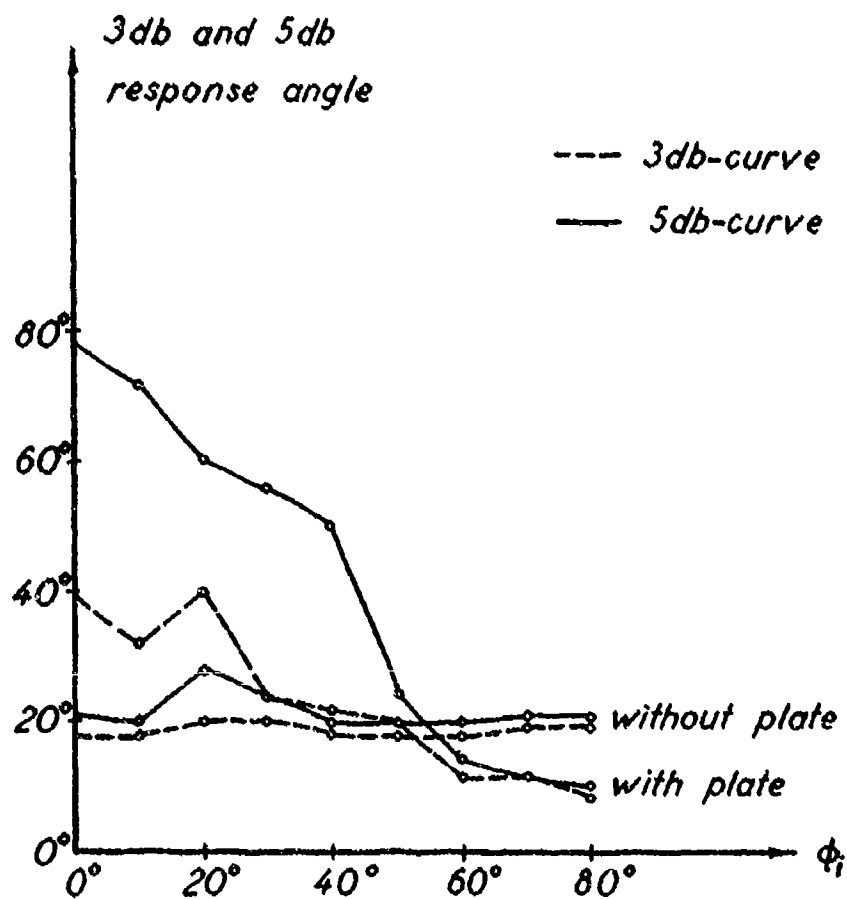


Fig.13. Response angle coverage for 16 element Van Atta reflector with or without a plate.

*$d = 0.6 \lambda$, $a = 0.41 \lambda$, $h = 0.25 \lambda$, $Z_0 = 73$ ohms,
 $\nu = 90^\circ$.*

~~Unclassified~~
Security Classification

DOCUMENT CONTROL DATA - R&D

(Security classification of title, body of abstract and indexing annotation must be entered when the overall report is classified)

1. ORIGINATING ACTIVITY (Corporate author) Laboratory of Electromagnetic Theory Technical University of Denmark Lyngby, Denmark		2a. REPORT SECURITY CLASSIFICATION Unclassified	
		2b. GROUP	
3. REPORT TITLE SQUARE VAN ATTA REFLECTOR WITH OR WITHOUT A CONDUCTING PLATE			
4. DESCRIPTIVE NOTES (Type of report and inclusive dates) Scientific Report No. 5			
5. AUTHOR(S) (Last name, first name, initial) Larsen, Tove and Nielsen, Erik Drage			
6. REPORT DATE 31 August 1966	7a. TOTAL NO. OF PAGES 31	7b. NO. OF REFS 10	
8a. CONTRACT OR GRANT NO. AF 61(052)-794	9a. ORIGINATOR'S REPORT NUMBER(S) S127 R53		
b. PROJECT NO. 4600	9b. OTHER REPORT NO(S) (Any other numbers that may be assigned this report)		
c. Task No. 460010			
10. AVAILABILITY/LIMITATION NOTICES			
11. SUPPLEMENTARY NOTES		12. SPONSORING MILITARY ACTIVITY European Office of Aerospace Research Shell Building, 47 Cantersteen Brussels, Belgium.	
13. ABSTRACT A theoretical investigation of a square Van Atta reflector consisting of half wave dipoles mounted above and parallel to a conducting plate has been carried out. Each pair of antenna elements is represented by an equivalent circuit, using x-circuits for the transmissionlines. The mutual impedance between the antenna elements and the reradiation both from the elements and from the plate is taken into account. The influence of the conducting plate is treated by using the theory of images. The scattering cross section of the reflector has been examined analytically and numerically. The numerical results are compared with experimental results obtained by others.			

DD FORM 1473
1 JAN 64

Unclassified
Security Classification